PHYSICAL REVIEW B **80**, 241410(R) (2009)

# Shape-tunable electronic properties of monohydride and trihydride [112]-oriented Si nanowires

Abraham Hmiel and Yongqiang Xue*
*College of Nanoscale Science and Engineering, State University of New York, Albany, New York 12203, USA*
(Received 19 September 2009; revised manuscript received 24 November 2009; published 16 December 2009)

Using first-principles calculations within density-functional theory, we demonstrated shape-dependent electronic properties of [112]-oriented Si nanowires (SiNWs) with monohydride (mh-SiNW) and trihydride (th-SiNW) passivation. We show for both mh-SiNWs and th-SiNWs, an indirect-to-direct band-gap transition can be induced solely by varying the cross-sectional aspect ratio of the {111} and {110} facets enclosing the nanowires, which is explained by the different confinement effects on the conduction-band state at Γ point by the two facets. For both mh-SiNWs and th-SiNWs, the hole (electron) effective mass converges to a value independent of cross-sectional area (aspect ratio). By analyzing the formation energy, we show that direct band-gap [112] SiNWs are possible to form at experimentally relevant passivation conditions.

DOI: 10.1103/PhysRevB.80.241410 PACS number(s): 79.60.Jv, 62.23.Hj, 71.20.−b

Silicon nanowires (SiNWs) have been studied extensively in recent years as promising building blocks for future nanoscale electronic, thermoelectric, and electromechanical devices due to their compatibility with current semiconductor technology.[1] The interests in SiNWs also arise from their electronic and optical properties due to quantum confinement, which can be modified through precise control of the growth orientation, surface passivation, and nanowire stoichiometry during fabrication processes. The production of H-terminated SiNWs in the diameter range of 1–5 nm in bulk quantities[2,3] has stimulated a number of computational studies on the structure-property relationship of these quasi-1D (one dimensional) nanostructures.[4–6] An important observation, of relevance to the development of Si-based photonic devices, is the possibility of obtaining direct band gap for small diameter SiNWs of different growth orientation, which deviates considerably from the bulk Si.

The confinement-induced direct band-gap formation in H-passivated SiNWs can be understood from the folding of the bulk Si band. For [100] and [110] SiNWs, parts of the six equivalent conduction-band minima can be projected onto the Γ point of the 1D Brillouin zone with an upward shift in energy level induced by confinement. The amount of up shift is smaller than that of the projection of the remaining conduction-band minima because of the larger effective mass in the confinement plane, leading to a direct band gap significantly larger than that of the bulk Si at decreasing wire diameter.[4,5] In contrast, for [111] and [112] SiNWs, there is no conduction-band minima which can be projected onto the Γ point. They are thus expected to exhibit an indirect band gap at large diameters. Previous work has shown that an indirect-to-direct band transition can occur for [111] SiNWs as diameter decreases to $\leq 2$ nm, but the difference between the indirect and direct gaps remains small.[4,5] Much less attention has been paid to [112] SiNWs,[7] although they are the most abundant SiNWs grown by the oxide-assisted growth process.[2] In addition, most previous studies considered just SiNWs with heuristically chosen structures, paying less attention to the many possible facet configurations and cross-sectional shapes.[3]

Recent computational study combining genetic algorithm optimization with density-functional theory (DFT) (Ref. 8) has shown that the H-terminated [112] SiNWs can take stable structures with a rectangular cross section bounded by monohydride {110} and {111} facets with dihydride bridges at the corner or the {111} facets may acquire trihydride termination, although only the trihydride [112] SiNWs have been experimentally observed and experimental measurements of band gap are available for them.[2] Two recent works[9,10] have suggested that an indirect-to-direct band transition for monohydride [112] SiNWs may be induced by varying the cross-sectional aspect ratio, which call for further study. In this Rapid Communication, we present a systematic first-principles investigation on the shape-tunable electronic properties of the [112] SiNWs for both monohydride (mh-SiNWs) and trihydride (th-SiNWs) passivation.

Our DFT calculations are performed using the SIESTA code[11] with the Perdew-Burke-Ernzerhof functional within the generalized gradient approximation (Ref. 12) and norm-conserving pseudopotential.[13] We used the double-zeta plus polarization optimized basis set and a real-space mesh cutoff of 350 Ry. A vacuum region of at least 13 Å is employed in the lateral directions to eliminate the interaction between the image SiNWs in neighboring cells within the supercell method. The Brillouin zone was sampled using a $1\times1\times24$ Monkhorst-Pack $k$-point mesh. Structure relaxations are performed to reduce the force on each atom to below 0.01 eV/Å. The lattice constant along the wire axis (chosen as the $z$ axis) is optimized by minimizing the uniaxial stress (6.611–6.617 Å for mh-SiNWs and 6.644–6.675 Å for th-SiNWs). Although it is well known that the DFT calculations systematically underestimate the band gap, recent quasiparticle calculation using the GW approximation for SiNWs,[4] which is computationally expensive, has indicated that the general trend of band-gap variation and band dispersion close to the gap region are well reproduced by the DFT calculations. This makes possible a reliable investigation on the indirect-to-direct band transition for [112] SiNWs with moderate computational costs.

We use the notation $A_nB_m$ to classify the [112] SiNWs of different shape, where the labels $A$ and $B$ represent the {111} and {110} facets, respectively, while the indices $n$ and $m$ characterize the number of layers parallel to the {111} and {110} facets (see Fig. 1). The wires studied here correspond to $n=2-7$ and $m=2-5$. The cross-sectional aspect ratio is defined as the ratio between the lateral dimension of the

 

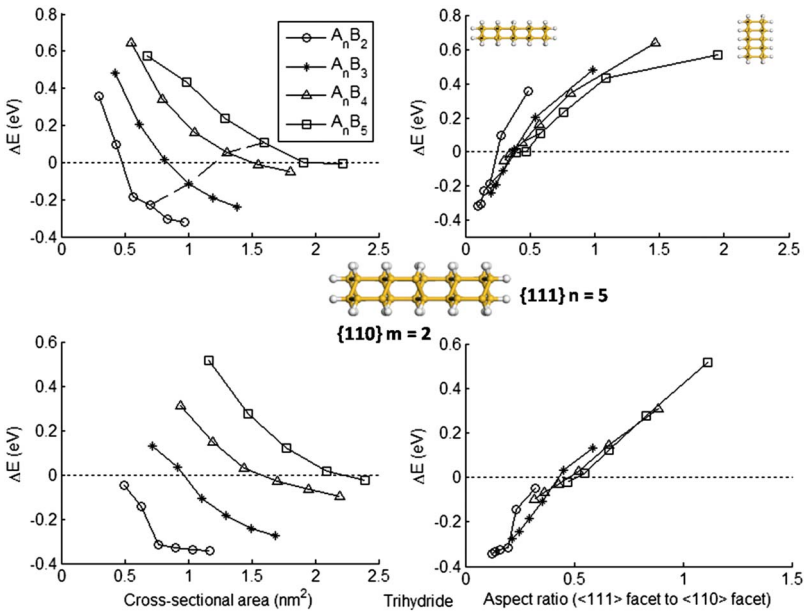


FIG. 1. (Color online) Indirect-direct band-gap difference Δ versus cross-sectional area (left figure) and aspect ratio (right figure) for monohydride (upper figure) and trihydride (lower figure) [112] SiNWs. The geometry of the SiNWs is denoted $A_nB_m$ and characterized by the number of layers $n$ ($m$) parallel to the {111} ({110}) facet. The dashed line represents the nanowire series of $A_5B_m$, $B=2-5$. The inset shows the top view of the atomic structure of the monohydride $A_5B_2$ SiNW. The horizontal line at $\Delta=0$ denotes indirect-to-direct transition.

{111} and {110} facets projected onto the $xy$ plane. An increasing aspect ratio thus correlates with an increasing ratio of $m/n$. For all the [112] SiNWs studied, the valence-band maximum (VBM) is located at the Γ point. To quantify the indirect to direct band-gap transition, we define an energy difference Δ between the energy of conduction-band bottom at the Γ point and the conduction-band minimum near the Brillouin-zone boundary ($X$ point). Therefore, a positive (negative) Δ denotes indirect (direct) band gap with indirect-to-direct transition occurring at $\Delta=0$.[9]

The shape-induced indirect-to-direct band transition is shown clearly in Fig. 1, where we plot four series of [112] SiNWs corresponding to $A_nB_2$,$A_nB_3$,$A_nB_4$ and $A_nB_5$ for both monohydride and trihydride passivation, where $n=2-7$. The same set of data points could also be plotted with the indices exchanged, e.g., the dashed line in the monohydride plot represents the nanowire series of $A_5B_m$ with $m=2$, 3, 4, 5. For both monohydride and trihydride passivations, the [112] SiNWs exhibit a direct band gap at decreasing {111} to {110} facet ratio with the transition point occurring at ~0.5, independent of the cross-sectional area. Although similar indirect-to-direct transition for mh-SiNWs was observed by Lu *et al.*,[9] these authors attributed the transition mechanism to the different contribution to conduction-band density of states by the Si atoms on the {111} and {110} facets. Since the trihydride passivation of the {111} facets modifies substantially the facet atomic structure, the similar pattern of indirect-to-direct transition for mh-SiNWs and th-SiNWs suggests instead a mechanism based on the contribution from the interior atoms. This is further evidenced by examining the electron/hole effective masses as a function of the cross-sectional area and aspect ratio for both mh-SiNWs and th-SiNWs. As shown in Fig. 2, we found that the electron effective masses for both mh-SiNWs and th-SiNWs converge

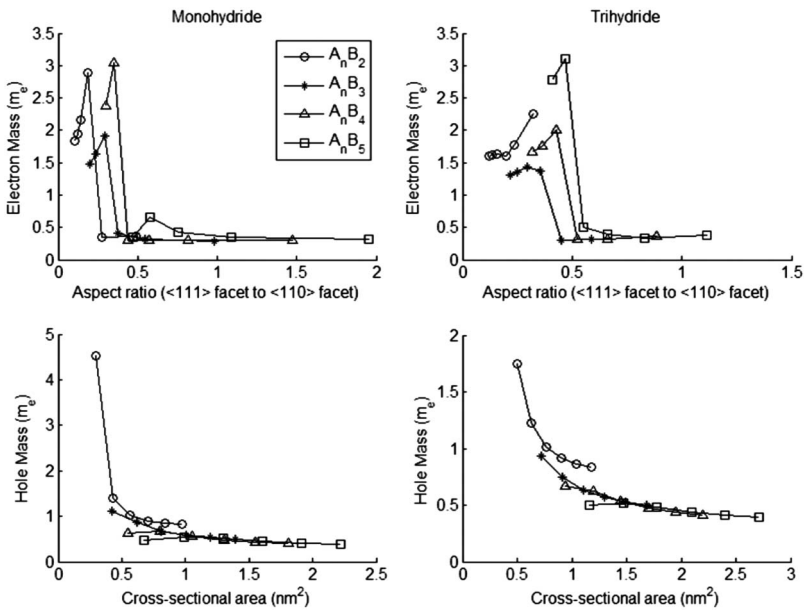


FIG. 2. Electron (upper figure) and hole (lower figure) effective masses for mh-SiNWs and th-SiNWs. For both mh-SiNWs and th-SiNWs, the hole (electron) effective masses converge to essentially identical values at increasing cross-sectional area (aspect ratio).

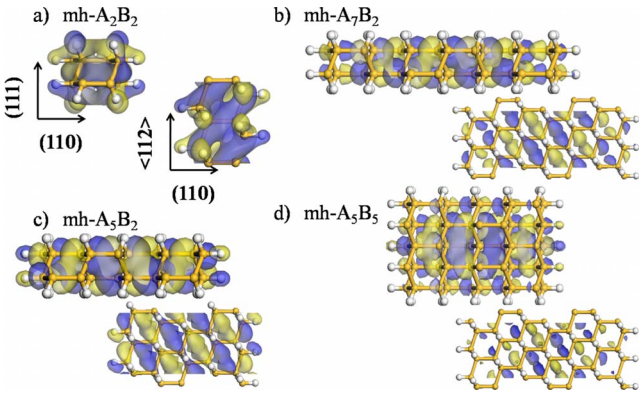


FIG. 3. (Color online) Wave-function plots for monohydride $A_2B_2$ (a), $A_7B_2$ (b), $A_5B_2$ (c), and $A_5B_5$ (d) SiNWs corresponding to conduction-band bottom at Γ point. For each mh-SiNW, we show both the top view (upper figure) and side view (lower figure) of the wave function. The blue and darker (yellow and lighter) region represents the positive (negative) part of the wave function. Going from $A_2B_2$ (a) to $A_7B_2$ (b), the wave function extends further in the confinement direction corresponding to the {111} facet and the SiNWs change from indirect to direct band gap. Going from $A_5B_2$ (c) to $A_5B_5$ (d), the wave function extends further in the confinement direction corresponding to the {110} facet and the SiNWs change from direct to indirect band gap.

to essentially identical values at increasing aspect ratio, corresponding to the indirect band-gap region. But the hole effective masses for both mh-SiNWs and th-SiNWs converge to essentially identical values with increasing cross-sectional area, independent of the aspect ratio.

Examining the electronic band-structure variations across the different series of SiNWs shows that the energy levels of the conduction-band minimum close to the Brillouin-zone boundary change only a little relative to the VBM. To reveal the mechanism of the observed indirect-to-direct transition, we analyze therefore the nature of the wave function of the conduction-band bottom at the Γ point. In Fig. 3, we show the wave-function plots for four mh-SiNWs, corresponding to the beginning ($A_2B_2$) and end ($A_7B_2$) of the series $A_nB_2$ and the beginning ($A_5B_2$) and end ($A_5B_5$) of the series $A_5B_m$. The wave-function plots for the corresponding th-SiNWs show similar distribution. We found that the wave functions of the conduction-band bottom at Γ point arise from hybridized $p$ orbitals of the interior Si atoms and extend within the plane perpendicular to the {110} facets. The sign of the wave function alternates between neighbor layers in the direction perpendicular to {110} facets but does not change between neighbor layers in the direction perpendicular to the {111} facets. This leads to an antibonding configuration in the confinement direction corresponding to {110} facets but a bonding configuration in the confinement direction corresponding to {111} facets. Therefore, as we move from $A_2B_2$ to $A_7B_2$, the wave function extends further in the confinement direction due to the {111} facets leading to down shift in the energy level of conduction-band bottom at Γ point, and the SiNWs change from indirect to direct band gap. As we move from $A_5B_2$ to $A_5B_5$, the wave function extends further in the confinement direction due to the {110} facets leading to up shift in the energy level of conduction-band bottom at Γ point, and the SiNWs change from direct to indirect band gap. Since the confinement effect of the {110} facets is stronger than that of the {111} facets for the given wave-function shape, the SiNWs will move to the indirect band-gap region when the number of layers ($m$) parallel to the {110} facet is sufficiently large, and the energy difference Δ eventually converges to a value close to the difference between the direct and indirect band gap obtained from the bulk Si band structure projected onto the [112] direction. The last series $A_nB_5$ in Fig. 1 show clearly this trend. In contrast, the wave function corresponding to the VBM at Γ point for both mh-SiNWs and th-SiNWs was found to arise from hybridized $sp^3$ orbitals extending along the Si-Si bond and is delocalized throughout the interior Si atoms. This explains why the hole effective mass converges to essentially identical values with increasing cross-sectional area for both mh-SiNWs and th-SiNWs.

The nature of the wave function of conduction-band bottom at Γ point also explains the strain dependence of the [112] SiNWs band structure. Examining the variation in the wave function along the nanowire axis shows a bonding configuration for the conduction-band state at Γ point between neighbor unit cells, with no nodal plane perpendicular to the axial direction. When applying a compressive uniaxial strain, which reduces the lattice constant, we expect a down shift in the energy level of the conduction-band bottom at Γ point, leading to a reduced energy difference Δ. For the case of monohydride [112] SiNWs, this was indeed observed by Huang *et al.*[10] Our results here also suggest that a similar scenario could apply to the th-SiNWs. In addition, a careful examination of the indirect-to-direct band-gap transition plotted in Fig. 1 reveals subtle differences between mh-SiNWs and th-SiNWs. As we vary along the series from $A_2B_m$ to $A_7B_m$ for $m=2-5$, the energy difference Δ changes with a larger amount for the monohydride SiNWs as the number of layers $n$ parallel to the {111} facets increases. But as we vary along the series from $A_nB_2$ to $A_nB_5$ for $n=2-7$ (as indicated by the dashed line in Fig. 1 where $n=5$), the energy difference Δ changes instead with a larger amount for the trihydride SiNWs as the number of layers $m$ parallel to the {110} facets increases. This is because that trihydride passivation occurs only at the {111} facets. The strong H-Si bonds at the trihydride {111} facets weaken the Si-Si bond and leads to a slightly larger Si-Si bond length perpendicular to the {111} facets, which in turn induces a slightly shorter Si-Si bond length perpendicular to the {110} facets. Consequently, the confinement effect due to the {110} ({111}) facets is stronger for the th-SiNWs (mh-SiNWs) leading to larger variation in Δ as the number of layers $m(n)$ parallel to the {110} ({111}) facets increases.

To determine the relative stability of the [112] SiNWs of different shape and surface passivation, we calculated the formation energy Ω as a function of the hydrogen chemical potential $\mu_H$ following Northrup[14]

$$\Omega = E^{tot} + E_{ZPE} - n_{Si}\mu_{Si} - n_H\mu_H, \quad (1)$$

where $E^{tot}$ is the total energy of SiNWs, $E_{ZPE}$ is the zero-point energy of Si-H vibrations, and $n_{H(Si)}$ is the number of H

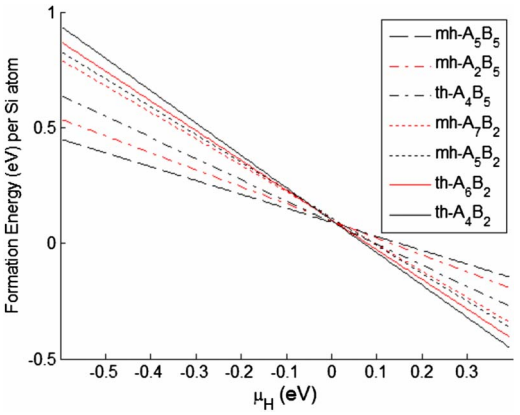


FIG. 4. (Color online) Relative stabilities of [112] SiNWs: the formation energies per Si atom for four mh-SiNWs and three th-SiNWs were plotted as a function of the hydrogen chemical potential. To aid visualization, the ordering of the labels from top to bottom in the legend has been chosen to coincide with the ordering of the formation energy at large H chemical potential $\mu_H$.

(Si) atoms.[15] We use the bulk energy for $\mu_{Si}$ and measure $\mu_H$ relative to the value, where the $SiH_4$ molecule can be formed from a reservoir of H and bulk Si without energy cost.[14] We calculated the Si-H vibrational frequency from a series of cluster calculations mimicking the atomic structure of the passivated [112] SiNWs using GAUSSIAN 03 code,[16] the result of which converges quickly with increasing cluster size. Representative results for both mh-SiNWs and th-SiNWs from the two series $A_nB_2$ and $A_nB_5$ are shown in Fig. 4, which confirm that direct band-gap [112] SiNWs can be more stable at higher H chemical potential. Specifically, the direct band-gap trihydride $A_4B_2/A_6B_2$ and monohydride $A_5B_2/A_7B_2$ SiNWs have lower formation energy than the indirect band-gap trihydride $A_4B_5$ and monohydride $A_2B_5/A_5B_5$ SiNWs at higher H chemical potential. These high $\mu_H$ conditions exist when the SiNWs are exposed to atomic H generated from $H_2$ gas at appropriate growth conditions or by HF etching.[17] Note that although the {110} facet was found to be energetically less favorable to form than {111} facet from the total-energy $E^{tot}$ calculations,[3,9] our calculation of formation energy $\Omega$ shows that it is possible to achieve [112] SiNWs with predominantly {110} facets at experimentally relevant passivation environments.

In conclusion, we have shown using first-principles DFT calculation that an indirect-to-direct band-gap transition can be induced in both monohydride and trihydride [112] SiNWs solely by varying the cross-sectional aspect ratio, which is caused by the different confinement effects on the conduction-band state at $\Gamma$ point from the {111} and {110} facets enclosing the nanowire. Analyzing the formation energy shows that direct band-gap [112] SiNWs can be more favorable to form at high H chemical potentials.

This work was supported by the SRC/DARPA Focus Center Research Programs.

*http://www.albany.edu/~yx152122

[1] Y. Huang, X. Duan, Y. Cui, L. Lauhon, K. Kim, and C. M. Lieber, Science **294**, 1313 (2001); A. I. Boukai, Y. Bunimovich, J. Tahir-Kheli, J.-K. Yu, W. A. Goddard III, and J. R. Heath, Nature (London) **451**, 168 (2008); R. He and P. Yang, Nat. Nanotechnol. **1**, 42 (2006).

[2] D. D. D. Ma, C. S. Lee, F. C. K. Au, S. Y. Tong, and S. T. Lee, Science **299**, 1874 (2003).

[3] R. Q. Zhang, Y. Lifshitz, D. D. D. Ma, Y. L. Zhao, Th. Frauenheim, S. T. Lee, and S. Y. Tong, J. Chem. Phys. **123**, 144703 (2005).

[4] X. Zhao, C. M. Wei, L. Yang, and M. Y. Chou, Phys. Rev. Lett. **92**, 236805 (2004); J.-A. Yan, L. Yang, and M. Y. Chou, Phys. Rev. B **76**, 115319 (2007).

[5] T. Vo, A. J. Williamson, and G. Galli, Phys. Rev. B **74**, 045116 (2006).

[6] P. W. Leu, B. Shan, and K. Cho, Phys. Rev. B **73**, 195320 (2006); M. F. Ng, L. Zhou, S. W. Yang, L. Y. Sim, V. B. C. Tan, and P. Wu, *ibid.* **76**, 155435 (2007); K.-H. Hong, J. Kim, S.-H. Lee, and J. K. Shin, Nano Lett. **8**, 1335 (2008); D. Yao, G. Zhang, G.-Q. Lo, and B. Li, Appl. Phys. Lett. **94**, 113113 (2009).

[7] H. Scheel, S. Reich, and C. Thomsen, Phys. Status Solidi B **242**, 2474 (2005); B. Aradi, L. E. Ramos, P. Deák, Th. Köhler, F. Bechstedt, R. Q. Zhang, and Th. Frauenheim, Phys. Rev. B **76**, 035305 (2007); R. Rurali, B. Aradi, Th. Frauenheim, and A. Gali, *ibid.* **76**, 113303 (2007).

[8] N. Lu, C. V. Ciobanu, T.-L. Chan, F.-C. Chuang, C.-Z. Wang, and K.-M. Ho, J. Phys. Chem. C **111**, 7933 (2007).

[9] A. J. Lu, R. Q. Zhang, and S. T. Lee, Appl. Phys. Lett. **92**, 203109 (2008).

[10] L. Huang, N. Lu, J.-A. Yan, M. Y. Chou, C.-Z. Wang, and K.-M. Ho, J. Phys. Chem. C **112**, 15680 (2008).

[11] J. M. Soler, E. Artacho, J. D. Gale, A. García, J. Junquera, P. Ordejón, and D. Sánchez-Portal, J. Phys.: Condens. Matter **14**, 2745 (2002).

[12] J. P. Perdew, K. Burke, and M. Ernzerhof, Phys. Rev. Lett. **77**, 3865 (1996).

[13] N. Troullier and J. L. Martins, Phys. Rev. B **43**, 1993 (1991).

[14] J. E. Northrup, Phys. Rev. B **44**, 1419 (1991); S. Hong and M. Y. Chou, *ibid.* **57**, 6262 (1998).

[15] R. Rurali and X. Cartoixà, Nano Lett. **9**, 975 (2009).

[16] M. J. Frisch *et al.*, GAUSSIAN 03, Revision D.02, Gaussian, Inc., Wallingford, CT, 2005.

[17] Y. Wu, Y. Cui, L. Huynh, C. J. Barrelet, D. C. Bell, and C. M. Lieber, Nano Lett. **4**, 433 (2004); G. Belomoin, J. Therrien, and M. Nayfeh, Appl. Phys. Lett. **77**, 779 (2000).